PHYSICAL REVIEW D **82,** 014023 (2010)

QCD critical point in a quasiparticle model

P. K. Srivastava, S. K. Tiwari, and C. P. Singh*

Department of Physics, Banaras Hindu University, Varanasi 221005, India

(Received 26 February 2010; published 30 July 2010)

Recent theoretical investigations have unveiled a rich structure in the quantum chromodynamics phase diagram, which consists of quark-gluon plasma and the hadronic phases but also supports the existence of a crossover transition ending at a critical end point (CEP). We find a too large variation in the determination of the coordinates of the CEP in the temperature (T) baryon chemical potential (μ_B) plane; and, therefore, its identification in the current heavy-ion experiments becomes debatable. Here we use an equation of state for a deconfined quark-gluon plasma using a thermodynamically-consistent quasiparticle model involving noninteracting quarks and gluons having thermal masses. We further use a thermodynamically-consistent excluded-volume model for the hadron gas, which was recently proposed by us. Using these equations of state, a first-order deconfining phase transition is constructed using Gibbs's criteria. This leads to an interesting finding that the phase transition line ends at a critical end point (CEP) beyond which a crossover region exists. Using our thermal hadron gas model, we obtain a chemical freeze out curve, and we find that the CEP lies in close proximity to this curve as proposed by some authors. The coordinates of CEP are found to lie within the reach of Relativistic heavy-ion collider experiment.

DOI: 10.1103/PhysRevD.82.014023 PACS numbers: 12.38.Mh, 12.38.Gc, 24.10.Pa, 25.75.Nq

I. INTRODUCTION

QCD, the non-Abelian gauge theory of strong interaction, predicts a phase transition between a hot and dense hadron gas (HG) and the quark gluon dominated phase, which is called as quark-gluon plasma (QGP) [1,2]. However, even after an intensive experimental as well as theoretical research spreading over the last two decades, our knowledge regarding the properties and signals of QGP is still very limited [3,4]. Even the phase boundary between the two phases remains in the literature as a conjectured one because the nonperturbative aspects of QCD are still dominant near the region close to the phase transition. In order to test the appearance of a deconfined QGP, which exists in a transient phase, we need a proper understanding of its subsequent hadronization process about which our knowledge is really very poor. The numerical method of lattice QCD can properly describe both the phases i.e., QGP and HG. However, lattice QCD studies have yielded results for finite and large values of temperature T and $\mu_B = 0$, and now we have surmounted difficulties in getting results for small, non vanishing values of μ_B [5,6]. Thus, we feel an urgent need to formulate a phenomenological model, which can successfully reproduce the lattice QCD data, and, hence, we can further use it to obtain the properties of QGP and to determine the QCD phase diagram in the entire (T, μ_B) plane.

In this paper, we present a thermodynamically self-consistent quasiparticle model of QCD, which describes a gas of quasiparticles with effective masses generated through the interactions among its basic constituents. This model has been found to work well above and around the critical temperature T_c. In order to describe the low energy HG phase, we work with our own model, which has been found in the past to give a proper description of the hot and dense HG [7]. The investigation of the structure of the QCD phase diagram has emerged as one of the most important and challenging topics in the nuclear and particle physics today. The precise determination of the phase boundary between QGP and HG at high temperature T and small μ_B has been a subject of intense research in recent years from experimental as well as theoretical points of view [8,9]. Lattice simulations first revealed that the transition between HG and QGP phase at $\mu_B = 0$ and large T is a crossover transition and there were further indications that the crossover transition turned into a first-order chiral phase transition for nonvanishing and finite values of μ_B [10]. Several attempts have since been made to locate precisely the critical end point (CEP) i.e., an ending point of the first-order chiral transition as μ_B decreases [11]. Although the existence of CEP was predicted a long time ago by a few lattice calculations, the absence of the CEP in the phase diagram was also noticed in some recent lattice calculations [12,13]. Thus, the location and the existence of the CEP in the phase diagram is still a matter of debate. Therefore, it is worthwhile to investigate the precise location of the CEP and to determine its properties in detail with the help of various phenomenological models [9]. However, confusion prevails since the coordinates of the CEP in the (T, μ_B) plane vary wildly in various models. Moreover, we are still not certain whether the conjectured phase boundary represents the chiral and/or deconfining phase transition line. Various calculations based on lattice QCD and/or effective models work with the basic assump-

*cpsingh_bhu@yahoo.co.in

tion that the finite μ_B chiral phase transition is first order, and, hence, the ending point of the line should automatically give the CEP, which is a second-order phase transition point. However, we know that the chiral symmetry is broken in the color-flavor locked (CFL) region which has extremely large values of μ_B. Theoretically, this topic has largely been investigated using several phenomenological models which can give results in the entire (T, μ_B) plane, whereas *ab initio* calculations are still limited to very small values in μ_B. However, all these efforts result in a very wide variation in the coordinates of the CEP [11]. In a recent paper, we proposed a new EOS for HG fireball where the geometrical size of the baryons in HG is explicitly incorporated as the excluded-volume correction in a thermodynamically-consistent manner [7]. Furthermore, we used a bag model EOS for the QGP phase and a first-order phase transition is constructed by equating pressures of both the phases using Gibbs's criteria. We thus obtain an interesting result that such a simple picture not only reproduces the entire conjectured phase boundary but the first-order phase transition line ends at a CEP beyond which a crossover region persists [7]. The coordinates of CEP as obtained in our calculation are found to be compatible with the prediction of a recent lattice gauge calculation of Gavai and Gupta [14]. Most importantly, we find here a deconfining phase transition in contrast to other calculations where the phase boundary depicts a chiral symmetry restoring phase transition. However, bag model is often a crude description to a gas of weakly interacting QGP, and the nonperturbative effect in this model arises from the pressure of the vacuum through the use of a phenomenological bag constant. In the present work, we consider QGP as a system of quasiparticles, which are quarks and gluons possessing temperature-dependent masses arising due to vacuum interactions [15–18]. Recently, these models are made thermodynamically self-consistent by incorporating suitable corrections in two different ways and, hence, are referred to as QPM I and QPM II in the following. Moreover, these descriptions were initially given for the gluon plasma only. We extend both the models for a QGP with finite baryon chemical potential μ_B, and we further assume their validity starting from a threshold temperature $T_0 = 100$ MeV below the critical temperature T_c, and we adjust the parameters of the models accordingly. We further compare their predictions for the energy density ϵ and the pressure p of the QGP with those obtained previously from the lattice simulation approach. Furthermore, we obtain a new EOS for the hot and dense HG as formulated in the previous paper and construct the phase boundary by equating the QGP pressure with that of HG pressure. We thus determine the critical parameters in the Gibbs's construction of a first-order deconfining phase transition. We draw the phase boundary line, and the end of the line determines the coordinates of the CEP. We also find the existence of a crossover transition lying beyond CEP. Finally, we compare our findings with those obtained in various other models.

The plan of the paper runs as follows. There are two types of quasiparticle models which are thermodynamically self-consistent. In Sec. II, we describe quasiparticles (QP), their corresponding equation of state, and discuss the criterion of thermodynamical consistency. In Sec. III, we describe the first thermodynamically-consistent quasiparticle model [15] of Gorenstein and Yang, the dependence of the quark and gluon masses on the temperature, and the extension of the model to describe the physics at finite μ_B. In Sec. IV, we discuss the second thermodynamically-consistent quasiparticle model [16] of Bannur and its extension for the finite μ_B. In Sec. V, we give our formulation for an excluded-volume model for the hot and dense hadron gas, and we discuss about its thermodynamical consistency. Section VI summarizes our results and discussions.

II. QUASIPARTICLE MODELS (QPM)

Quasiparticles are the thermal excitations of the interacting quarks and gluons. The quasiparticle model in QCD is a phenomenological model which is widely used to describe the nonideal behavior of QGP near the phase transition points. It was first proposed by Goloviznin and Satz [17] and then by Peshier *et al.* [18] to explain the EOS of QGP obtained from lattice gauge simulation of QCD at finite temperature. In quasiparticle models, the system of interacting massless quarks and gluons can be effectively described as an ideal gas of "massive" noninteracting quasiparticles. The mass of these quasiparticles is temperature dependent and arises because of the interactions of quarks and gluons with the surrounding matter in the medium. These quasiparticles retain the quantum numbers of the real particles i.e., the quarks and gluons. It was assumed that energy ω and momentum k of the quasiparticles obey a simple dispersion relation :

$$\omega^2(k, T) = k^2 + m^2(T), \tag{1}$$

where $m(T)$ is the temperature-dependent mass of the quasiparticle. The pressure and energy density of the ideal gas of quasiparticles are dependent on ω and $m(T)$ and are given by [15]

$$p_{\rm id}(T, m) = \mp \frac{Td}{2\pi^2}\int_0^\infty k^2 dk \ln\left[1 \mp \exp\left(-\frac{(\omega-\mu_q)}{T}\right)\right], \tag{2}$$

$$\epsilon_{\rm id}(T, m) = \frac{d}{2\pi^2}\int_0^\infty k^2 dk \frac{\omega}{[\exp(\frac{\omega-\mu_q}{T}) \mp 1]}, \tag{3}$$

where d represents the degeneracy factor for quarks and/or gluons. However, Gorenstein and Yang pointed out that this model involves a thermodynamical inconsistency [15]. It did not satisfy the fundamental thermodynamic relation:

$\epsilon(T) = T\frac{dp(T)}{dT} - p(T)$. So, they reformulated the statistical mechanics for a system whose constituents follow a medium-dependent dispersion relation, and the above inconsistency problem was handled by them by introducing a temperature-dependent vacuum energy term, which effectively cancelled the inconsistent term. Alternatively, Bannur also pointed out the reason for the above thermodynamical inconsistency [16]. If the particle mass in the system is not constant and it depends upon the medium, then the relation used between the pressure and grand canonical partition function does not hold good. So one can start from the definitions of the energy density and the average particle number density in the grand canonical ensemble formalism and in this way a different thermodynamically-consistent quasiparticle model for QGP can be obtained.

III. FIRST QUASIPARTICLE MODEL (QPM I)

Gorenstein and Yang initially formulated a thermodynamically-consistent quasiparticle model for a gluon plasma at $\mu_B = 0$, and later they extended it for the QGP having a finite value of μ_B. In this model, the effective mass of the gluon changes with T and μ_B as follows [15]:

$$m_g^2(T) = \frac{N_c}{6} g^2(T)T^2\left(1 + \frac{N_f'}{6}\right), \tag{4}$$

where N_c represents the number of colors. We have also taken $N_c = 3$ in our calculation. And

$$N_f' = N_f + \frac{3}{\pi^2}\sum_f \frac{\mu_f^2}{T^2}. \tag{5}$$

Here, N_f is the number of flavors of quarks and μ_f is the quark chemical potential belonging to the flavor f. Similarly, the effective mass of a quark of flavor f changes with T and μ_B as [19]

$$m_{qf}^2(T) = \frac{g^2(T)T^2}{6}\left(1 + \frac{\mu_f^2}{\pi^2 T^2}\right). \tag{6}$$

Here, $g^2(T)$ is the QCD running coupling constant. We have taken the following form for $g^2(T)$ [20,21]:

$$\begin{aligned}\alpha_S(T) &= \frac{g^2(T)}{4\pi}\\ &= \frac{6\pi}{(33 - 2N_f)\ln(\frac{T}{\Lambda_T}\sqrt{1 + a\frac{\mu_q^2}{T^2}})}\\ &\quad\times\left(1 - \frac{3(153 - 19N_f)}{(33 - 2N_f)^2}\frac{\ln(2\ln\frac{T}{\Lambda_T}\sqrt{1 + a\frac{\mu_q^2}{T^2}})}{\ln(\frac{T}{\Lambda_T}\sqrt{1 + a\frac{\mu_q^2}{T^2}})}\right),\end{aligned} \tag{7}$$

where Λ_T is the QCD scale-fixing parameter, which characterizes the strength of the interaction. We have taken $\Lambda_T = 115$ MeV in our calculation. Here, parameter a is equal to $\frac{1}{\pi^2}$ [22].

After reformulating the statistical mechanics and incorporating the additional medium contribution, the pressure p and energy density ϵ for a system of quasiparticles can be written in a thermodynamically-consistent manner as follows [15,18]:

$$p(T, m) = p_{\rm id} - B(T, \mu_B), \tag{8}$$

$$\epsilon(T, m) = \epsilon_{\rm id} + B(T, \mu_B). \tag{9}$$

The first term on the right hand side of both the equations is the standard ideal gas expression given by Eq. (1) and (2), respectively. The second term represents the medium contribution:

$$B(T, \mu_B) = \lim_{V\to\infty}\frac{E_0}{V}, \tag{10}$$

where E_0 is the vacuum energy in the absence of quasiparticle excitations or zero point energy. However, this energy term is not a constant but depends upon μ_B and T. The $B(T, \mu_B)$ can be derived as follows [23]:

$$\begin{aligned}B(T, \mu_B) = B_0 - \frac{d}{4\pi^2}\int_{T_0}^{T} dT\frac{dm^2(T)}{dT}\int_0^\infty \frac{k^2 dk}{\omega}\\ \times\frac{1}{[\exp(\frac{\omega-\mu_q}{T})] \mp 1},\end{aligned} \tag{11}$$

where B_0 is the integration constant i.e., the value of $B(T, \mu_B)$ at $T = T_0$. The expression for $B(T, \mu_B)$ in Eq. (11) and the forms of Eqs. (8)–(10) give a compelling evidence that $B(T, \mu_B)$ may be treated as T and μ_B-dependent bag constant term [24]. In our calculation we take $B_0^{1/4} = 185$ MeV and $T_0 = 100$ MeV. We have also taken $\mu_B = 3\mu_q$.

IV. SECOND QUASIPARTICLE MODEL (QPM II)

The second thermodynamically-consistent quasiparticle model is given by Bannur [16]. Bannur first figured out why there exists a thermodynamical inconsistency in the quasiparticle description of Peshier *et al.* The relation between pressure and grand canonical partition function cannot hold good if the particles of the system have a temperature-dependent mass. So he used the definition of average energy and average number of particles and derived all the thermodynamical quantities from them in a consistent manner. In this model, the effective mass of the gluon is the same as given in Eq. (4). However, the effective mass of the quarks involves the following relation:

$$m_q^2 = m_{q0}^2 + \sqrt{2}m_{q0}m_{\rm th} + m_{\rm th}^2, \tag{12}$$

where m_{q0} is the rest mass of the quarks. In this calculation, we have used $m_{q0} = 8$ MeV for two light quarks (u, d) and $m_{q0} = 80$ MeV for strange quark. In the above Eq. (12) $m_{\rm th}$ represents the thermal mass of the quarks and it can be written as [23]

$$m_{\rm th}^2(T,\mu) = \frac{N_c^2-1}{8N_c}\left[T^2 + \frac{\mu_q^2}{\pi^2}\right]g^2(T). \tag{13}$$

Taking these values for the effective masses, energy density can be derived from the grand canonical partition function in a thermodynamically-consistent manner and is given as

$$\epsilon = \frac{T^4}{\pi^2}\sum_{l=1}^{\infty}\frac{1}{l^4}\left[\frac{d_g}{2}\epsilon_g(x_g l) + (-1)^{l-1}d_q\cosh(\mu_q/T)\epsilon_q(x_q l) + (-1)^{l-1}\frac{d_s}{2}\epsilon_s(x_s l)\right], \tag{14}$$

with $\epsilon_i(x_i l) = (x_i l)^3 K_1(x_i l) + 3(x_i l)^2 K_2(x_i l)$, where K_1 and K_2 are the modified Bessel functions, with $x_i = \frac{m_i}{T}$ and index i runs for gluons, up-down quarks q, and strange quark s. Here, d_i are the degeneracies associated with the internal degrees of freedom. Now, by using the thermodynamic relation $\epsilon = T\frac{\partial p}{\partial T} - p$, pressure of system at $\mu_q = 0$ can be obtained as

$$\frac{p(T,\mu_q=0)}{T} = \frac{p_0}{T_0} + \int_{T_0}^{T} dT\frac{\epsilon(T,\mu_q=0)}{T^2}, \tag{15}$$

where p_0 is the pressure at a reference temperature T_0. We have used $p_0 = 0$ at $T_0 = 100$ MeV in our calculation. Using the relation between the number density n_q and the grand canonical partition function, we can get the pressure for a system at finite μ_B:

$$p(T,\mu_q) = p(T,0) + \int_0^{\mu_q} n_q d\mu_q, \tag{16}$$

where the expression for n_q can be given as follows:

$$n_q = \frac{d_q T^3}{\pi^2}\sum_{l=1}^{\infty}(-1)^{l-1}\frac{1}{l^3}\sinh(\mu_q/T)I_i(x_i l) \tag{17}$$

with $I_i(x_i l) = (x_i l)^2 K_2(x_i l)$. Thus, all the thermodynamical quantities can be obtained in a consistent way by using this model.

V. EOS FOR A HADRON GAS

There is no deconfinement transition if the hadron gas consists of pointlike particles, and consequently HG pressure is always larger than QGP pressure. Therefore, inclusion of a repulsive interaction between two baryons having a hard-core size reduces the HG pressure, and, hence, it stabilizes the formation of QGP at high baryon densities. Recently we have proposed a thermodynamically-consistent excluded-volume model for hot and dense HG. In this model, the grand canonical partition function for the HG, with full quantum statistics and after incorporating excluded-volume correction, can be written as [25]

$$\ln Z_i^{\rm ex} = \frac{g_i}{6\pi^2 T}\int_{V_i^0}^{V-\sum_j N_j V_j^0} dV \int_0^\infty \frac{k^4 dk}{\sqrt{k^2+m_i^2}} \times \frac{1}{[\exp(\frac{E_i-\mu_i}{T})+1]}, \tag{18}$$

where g_i is the degeneracy factor of ith species of baryons, E_i is the energy of the particle ($E_i = \sqrt{k^2+m_i^2}$), V_i^0 is the eigenvolume of one baryon of ith species and $\sum_j N_j V_j^0$ is the total occupied volume, and N_j represents total number of baryons of jth species.

Now we can write Eq. (17) as

$$\ln Z_i^{\rm ex} = V\left(1 - \sum_j n_j^{\rm ex} V_j^0\right) I_i \lambda_i, \tag{19}$$

where I_i represents the integral

$$I_i = \frac{g_i}{6\pi^2 T}\int_0^\infty \frac{k^4 dk}{\sqrt{k^2+m_i^2}}\frac{1}{[\exp(\frac{E_i}{T})+\lambda_i]}, \tag{20}$$

and $\lambda_i = \exp(\frac{\mu_i}{T})$ is the fugacity of the particle; $n_j^{\rm ex}$ is the number density of jth type of baryons after excluded-volume correction and can be obtained from Eq. (18) as

$$n_i^{\rm ex} = \frac{\lambda_i}{V}\left(\frac{\partial \ln Z_i^{\rm ex}}{\partial \lambda_i}\right)_{T,V}. \tag{21}$$

This leads to a transcendental equation as

$$n_i^{ex} = (1-R)I_i\lambda_i - I_i\lambda_i^2\frac{\partial R}{\partial \lambda_i} + \lambda_i^2(1-R)I_i', \tag{22}$$

where I_i' is the partial derivative of I_i with respect to λ_i and $R = \sum_i n_i^{\rm ex} V_i^0$ is the fractional occupied volume. We can write R in an operator equation as follows [7]:

$$R = R_1 + \hat{\Omega} R, \tag{23}$$

where $R_1 = \frac{R^0}{1+R^0}$ with $R^0 = \sum n_i^0 V_i^0 + \sum I_i' V_i^0 \lambda_i^2$; n_i^0 is the density of pointlike baryons of ith species, and the operator $\hat{\Omega}$ has the form

$$\hat{\Omega} = -\frac{1}{1+R^0}\sum_i n_i^0 V_i^0 \lambda_i \frac{\partial}{\partial \lambda_i}. \tag{24}$$

Using Neumann iteration method and retaining the series up to $\hat{\Omega}^2$ term, we get

$$R = R_1 + \hat{\Omega}R_1 + \hat{\Omega}^2 R_1, \tag{25}$$

and Eq. (24) can be solved numerically. Finally, we get for the total pressure [25] of the hadron gas,

$$p_{\rm HG}^{\rm ex} = T(1-R)\sum_i I_i\lambda_i + \sum_i p_i^{\rm meson}. \tag{26}$$

In (26), the first term represents the pressure due to all types of baryons where excluded-volume correction is incorporated and the second term gives the total pressure due to all mesons in HG having a pointlike size. This makes it clear that we consider the hard-core repulsion arising between two baryons which possess a hard-core size. In this calculation, we have taken an equal volume $V^0 = \frac{4\pi r^3}{3}$ for each type of baryon with a hard-core radius $r = 0.8$ fm. We have taken all baryons and mesons and their resonances having masses up to 2 GeV/c^2 in our calculation for HG pressure. We have also used the condition of strangeness conservation by putting $\sum_i S_i(n_i^s - \bar{n}_i^s) = 0$, where S_i is the strangeness quantum number of the ith hadron and $n_i^s(\bar{n}_i^s)$ is the strange (antistrange) hadron density, respectively. Using this constraint equation, we get the value of strange chemical potential in terms of μ_B. We want to stress here that the form of this model used under Boltzmann approximation has been found to describe [26,27] very well the observed multiplicities and the ratios of the particles in heavy-ion collisions.

VI. RESULTS AND DISCUSSION

In order to demonstrate that both types of quasiparticle models reproduce the lattice results with the value of parameters chosen here, we show in Fig. 1 the results of our calculations for the variation of energy density with respect to temperature at different μ_B. We find that the predictions from both these models (QPM I and QPM II) compare well with the lattice data [28]. However, it cannot be regarded as a very good fit to the data. It is worthwhile to emphasize that our calculation involves two parameters Λ_T and T_0. We have used $T_0 = 100$ MeV and $\Lambda_T = 115$ MeV for a reasonable fit to the data. However, the effect of the change in values of the parameters on the curve is negligibly small. For example, if we take $\Lambda_T = 115$ MeV and $T_0 = 120$ MeV, there is no noticeable change in the predictions of both the models and the curve almost overlaps on the previous one as shown in Fig. 1. However, the curve with the parameter values $\Lambda_T = 100$ MeV and $T_0 = 100$ MeV lies slightly above the previous curve in both the models. Moreover, the results of QPM may improve if we use thermal gluon mass as $m_g^2(T) = g^2(T)T^2/3$ instead of $m_g^2(T) = g^2(T)T^2/2$ as pointed out by Bannur [16,21].

In Fig. 2, we have presented the results of our calculations for the QGP pressure p/T^4 in both the quasiparticle models and shown its temperature variation at different values of μ_B. We compare our results with those recently reported in lattice simulations [28,29]. We find that the fits by QPM II look slightly better than those given by QPM I. These results give us extreme confidence in both types of quasiparticle models being used as phenomenological models. Although, phenomenology cannot work as a substitute for a formal theory like QCD. Since the utility of lattice QCD calculations at very large μ_B is still not possible, we usually take the help of quasiparticle models in such circumstances. It is now widely used to describe the nonideal behavior of QGP observed near the critical line.

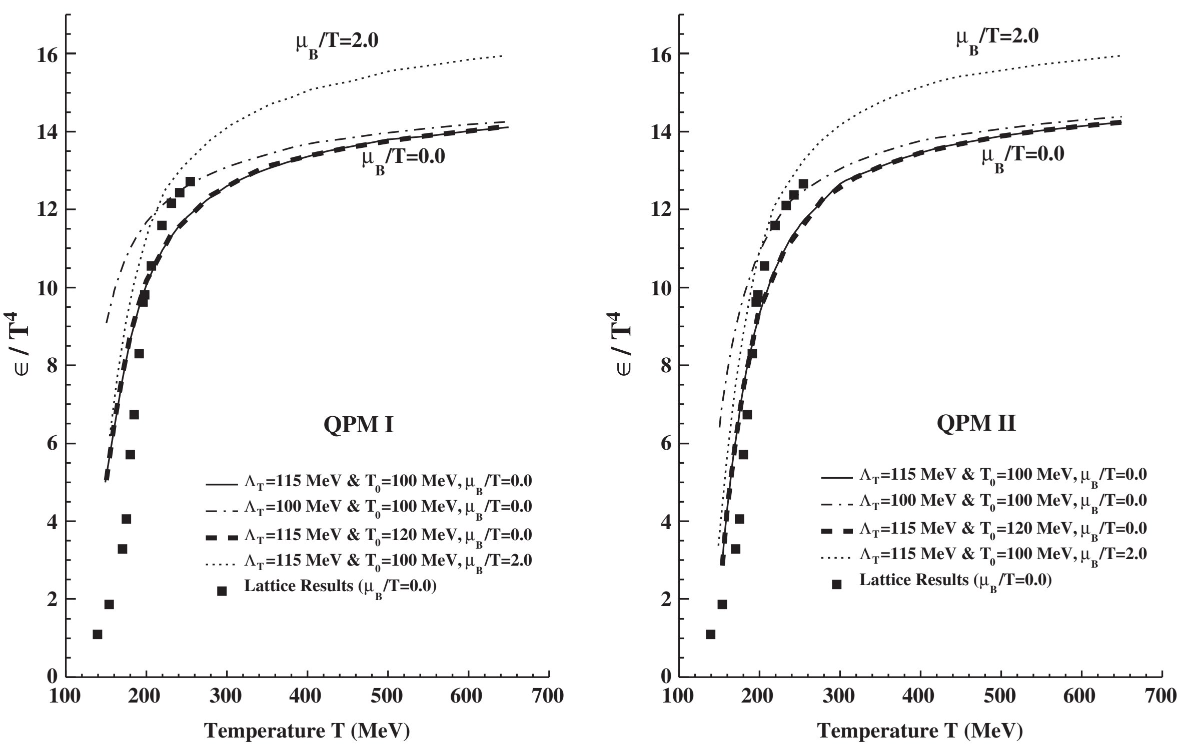

FIG. 1. Variation of ϵ/T^4 with temperature in Quasiparticle models. Left panel shows calculations based on the QPM I, and right panel demonstrates those of QPM II.

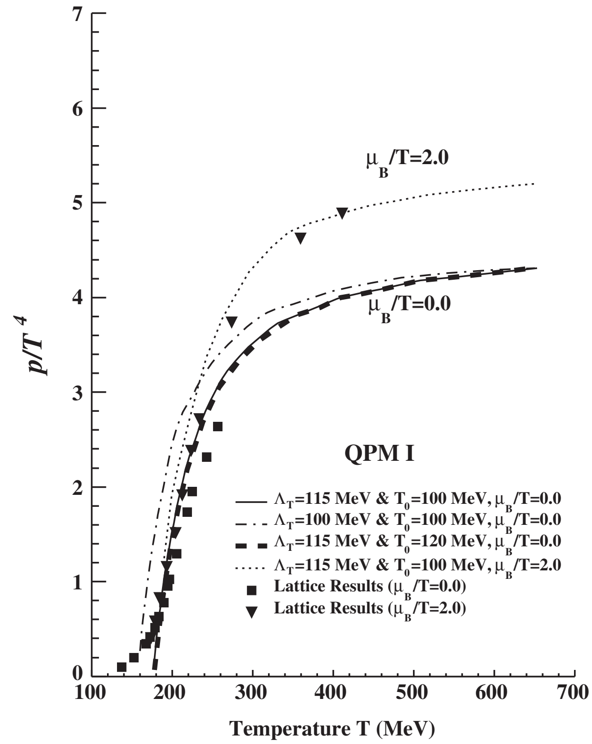

FIG. 2. The variation of p/T^4 with T in Quasiparticle models. The predictions of QPM I are shown in the left panel, and those of QPM II are shown in the right panel.

Moreover, we attempt to extend its uses at lower values of temperature, e.g., $T_0 < T_c$ (we take $T_0 = 100$ MeV). Usually, authors have studied the quasiparticle models above T_c only; and therefore, the rapid rise of pressure and energy density at or around T_c is not properly taken care of in these models. Our method of obtaining critical parameters (T_c, μ_c) involves the use of Gibbs's equilibrium criteria of equating HG and QGP pressures and to determine where these pressure lines intersect each other. Therefore, we want to know precisely the values of QGP pressure at temperatures $T_0(<T_c)$ also. The comparison of our calculations with the lattice results yields the required test about the suitability of quasiparticle EOS for QGP. In Fig. 2, we have again demonstrated how the changes in the parameter values affect the results. We find that $\Lambda_T = 115$ MeV and $T_0 = 120$ MeV yield a curve which overlaps with the curve obtained with $\Lambda_T = 115$ MeV and $T_0 = 100$ MeV. Similarly, if we use $\Lambda_T = 100$ MeV and $T_0 = 100$ MeV there is a slight change in the curve, but the overall effect is found to be small.

In Fig. 3, we have shown the phase boundary obtained in our model. Surprisingly, we again find here that the first-order deconfining phase transition line ends at a critical end point and the coordinates of CEP are ($T_{\rm CEP} = 183$ MeV, $\mu_{\rm CEP} = 166$ MeV) in QPM I and ($T_{\rm CEP} = 166$ MeV, $\mu_{\rm CEP} = 155$ MeV) in QPM II. It is interesting to find that the critical points obtained by us lie closer to CEP of

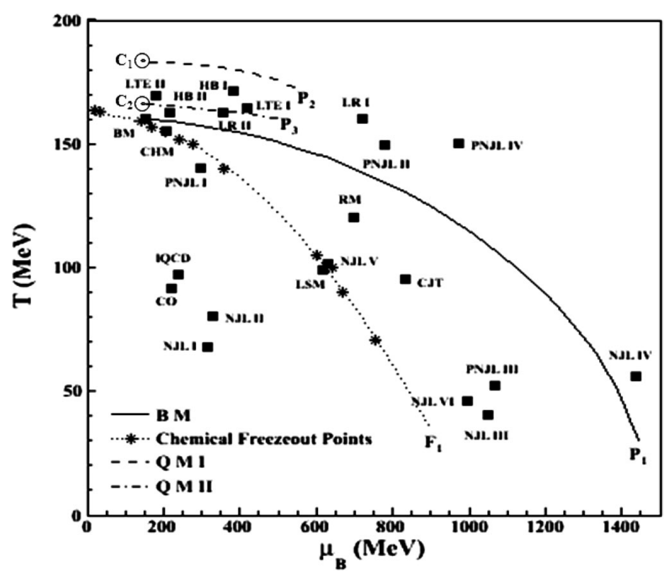

FIG. 3. The location of QCD critical point in QCD phase diagram. P_1 is the phase boundary in bag model (BM), P_2 is the phase boundary in QPM I, and P_3 is the phase boundary in QPM II. F_1 is the chemical freezeout line obtained using our HG model. C_1($T_{\rm CEP} = 183$ MeV, $\mu_{\rm CEP} = 166$ MeV) is the CEP on P_2 obtained in QPM I, and C_2($T_{\rm CEP} = 166$ MeV, $\mu_{\rm CEP} = 155$ MeV) is the CEP on P_3 obtained in QPM II. The labels used in the figure are explained in Table I.

some lattice calculations [14]. These points also compare well with the coordinates of CEP ($T_{\rm CEP} = 160$ MeV, $\mu_{\rm CEP} = 156$ MeV) obtained by us in the previous publication [7] using bag model calculation. Here, we would like to stress again that the changes in the parameter values ($\Lambda_T = 115$ MeV and $T_0 = 120$ MeV) do not show any appreciable change in the coordinates of CEP in both the models. However, the parameter values ($\Lambda_T = 100$ MeV and $T_0 = 100$ MeV) yield the new coordinates of CEP as ($T_{\rm CEP} = 166$ MeV, $\mu_{\rm CEP} = 155$ MeV) in the QPM I and ($T_{\rm CEP} = 152$ MeV, $\mu_{\rm CEP} = 151$ MeV) in QPM II, and these are small but noticeable changes. We also find a crossover region existing beyond the critical point where HG pressure, which is solely dominated by mesonic pressure term in Eq. (25), is always less than the QGP pressure. Therefore, no phase transition exists in this region. Since the temperature is much higher, the thermal fluctuations break mesonic constituents of HG into quarks, antiquarks, and gluons. We have tabulated in Table I the location of CEP obtained from various calculations for a comparison. For convenience, we have shown above the dark solid line all the values obtained in SU(3) flavor calculations. Below the solid line, the values of SU(2) are also shown in order to make the comparison complete.

We find that there exists a very wide variation in the coordinates of CEP obtained in different models. We notice that the critical end points obtained in the deconfining phase transition are usually located at $\mu_B < 200$ MeV, whereas chiral CEP have much larger μ_B. So there is a good chance for observing CEP at RHIC by using energy scan [47]. We also find that CEP obtained in our models almost overlaps with the points on the freeze out curve. The freeze out point occurs close to RHIC energy, and, hence, the fluctuations in multiplicity etc. can experimentally provide a clear signal for CEP.

Before we conclude, we would like to discuss the recent lattice data obtained by de Forcrand and Philipsen [12,13], who used 2 + 1 and 3 flavors, staggered fermions, and a Taylor expansion in μ_q/T to study the curvature of the critical surface at very light quark masses close to $\mu_q = 0$ surface. They noticed that the critical surface bends so that the first-order region shrinks at higher quark masses, and, hence, they conclude that there is no critical point at finite chemical potential. However, it is speculated that the critical surface bends back at larger μ_q, and the critical point may again reappear. In fact, a recent Nambu-Jona-Lassinio (NJL) model calculation lends support to this speculation [48].

In summary, we have demonstrated the occurrence of CEP in a deconfining first-order phase transition, constructed by using quasiparticle model for QGP and a new thermodynamically-consistent excluded-volume model for

TABLE I. Coordinates of CEP obtained in different models. The last column gives the corresponding label used in Fig. 3 and Ref. [11].

Source	($T_{\rm CEP}$, $\mu_{\rm CEP}$) MeV	Comments	Label
Present paper	(183, 166)	QPM I	C_1
Present paper	(166, 155)	QPM II	C_2
C. P. Singh *et al.* [7]	(160, 156)	Bag model	BM
Fodor and Katz [5]	(160, 725)	Lattice reweighting	LR I
Fodor and Katz [30]	(162, 360)	Lattice reweighting	LR II
S. Ejiri *et al.* [31]	(164, 420)	Lattice Taylor expansion	LTE I
Gavai and Gupta [14]	(166.2, 182.8)	Lattice Taylor expansion	LTE II
Antoniou and Kapoyannis [32]	(171, 385)	Hadronic bootstrap I	HB I
Antoniou *et al.* [33]	(162.1, 218.7)	Hadronic bootstrap II	HB II
Barducci *et al.* [34]	(91, 225)	Composite operator	CO
Barducci *et al.* [35]	(97, 240)	Ladder-QCD model	lQCD
D. Zschiesche *et al.* [36]	(155, 210)	Chiral hadron model	CHM
P. Costa *et al.* [37]	(67.7, 318.4)	SU(3) NJL	NJL I
M. Ciminale *et al.* [38]	(140, 300)	SU(3) Polyakov loop extended Nambu-Jona-Lasinio (PNJL)	PNJL I
P. Costa *et al.* [39]	(79.9, 331.72)	SU(2) NJL	NJL II
Asakawa and Yazaki [40]	(40, 1050)	SU(2) NJL	NJL III
Asakawa and Yazaki [40]	(55, 1440)	SU(2) NJL	NJL IV
Berger and Rajagopal [41]	(101, 633)	SU(2) NJL	NJL V
Scavenius *et al.* [42]	(46, 996)	SU(2) NJL	NJL VI
Scavenius *et al.* [42]	(99, 621)	Linear σ model	LSM
Kashiwa *et al.* [43]	(149, 783)	SU(2) PNJL + σ^4	PNJL II
Kashiwa *et al.* [43]	(52, 1071)	SU(2) PNJL + vector int.	PNJL III
S. Rößner *et al.* [44]	(150, 975)	SU(2) PNJL	PNJL IV
Halasz *et al*[45]	(120, 700)	Random matrix	RM
Hatta and Ikeda [46]	(95, 837)	Effective potential	CJT

hot and dense HG. In our model, we assign a hard-core volume for baryons, and mesons are treated as pointlike particles. So at higher temperatures, mesons can fuse into one another, but baryons occupy space. As μ_B increases, we find that the fractional occupied volume R by baryons increases, and, hence, the mobility of baryons decreases fast. The physical mechanism in our model is similar to the percolation model [49], where a first-order phase transition results due to *jamming* of baryons in the HG. Thus our finding lends support to the idea of realizing a phase transition by modelling the interactions existing in the HG in a suitable way.

ACKNOWLEDGMENTS

P. K. S. and S. K. T. are grateful to the University Grants Commission (UGC) and Council of Scientific and Industrial Research (CSIR), New Delhi. C. P. S. acknowledges the financial support through a project sanctioned by Department of Science and Technology, Government of India, New Delhi.

[1] C. P. Singh, Phys. Rep. **236**, 147 (1993); Int. J. Mod. Phys. A **7**, 7185 (1992).
[2] H. Satz, Rep. Prog. Phys. **63**, 1511 (2000).
[3] E. Shuryak, Prog. Part. Nucl. Phys. **62**, 48 (2009).
[4] H. Satz, Int. J. Mod. Phys. A **21**, 672 (2006).
[5] Z. Fodor and S. D. Katz, Phys. Lett. B **534**, 87 (2002); J. High Energy Phys. 03 (2002) 014.
[6] C. Schmidt, Proc. Sci., LAT2006 (2006) 021.
[7] C. P. Singh, P. K. Srivastava, and S. K. Tiwari, Phys. Rev. D **80**, 114508 (2009).
[8] M. A. Stephanov, Phys. Rev. Lett. **102**, 032301 (2009).
[9] M. A. Stephanov, Int. J. Mod. Phys. A **20**, 4387 (2005).
[10] M. A. Stephanov, K. Rajagopal, and E. V. Shuryak, Phys. Rev. Lett. **81**, 4816 (1998).
[11] M. A. Stephanov, Prog. Theor. Phys. Suppl. **153**, 139 (2004).
[12] P. de Forcrand and O. Philipsen, J. High Energy Phys. 01 (2007) 077.
[13] P. de Forcrand and O. Philipsen, J. High Energy Phys. 11 (2008) 012.
[14] R. V. Gavai and S. Gupta, Phys. Rev. D **71**, 114014 (2005).
[15] M. I. Gorenstein and S. N. Yang, Phys. Rev. D **52**, 5206 (1995).
[16] V. M. Bannur, Phys. Lett. B **647**, 271 (2007); J. Phys. G **32**, 993 (2006).
[17] V. Goloviznin and H. Satz, Z. Phys. C **57**, 671 (1993).
[18] A. Peshier, B. Kampfer, O. P. Pavlenko, and G. Soff, Phys. Rev. D **54**, 2399 (1996).
[19] H. Vija and M. H. Thoma, Phys. Lett. B **342**, 212 (1995).
[20] E. Braaten and R. D. Pisarski, Phys. Rev. D **45**, R1827 (1992).
[21] V. M. Bannur, Eur. Phys. J. C **50**, 629 (2007); Phys. Rev. C **78**, 045206 (2008); **75**, 044905 (2007).
[22] J. Letessier and J. Rafelski, Phys. Rev. C **67**, 031902(R) (2003).
[23] A. Peshier, B. Kampfer, and G. Soff, Phys. Rev. C **61**, 045203 (2000).
[24] B. K. Patra and C. P. Singh, Phys. Rev. D **54**, 3551 (1996); N. Prasad and C. P. Singh, Phys. Lett. B **501**, 92 (2001).
[25] C. P. Singh, B. K. Patra, and K. K. Singh, Phys. Lett. B **387**, 680 (1996); S. Uddin and C. P. Singh, Z. Phys. C **63**, 147 (1994).
[26] M. Mishra and C. P. Singh, Phys. Rev. C **76**, 024908 (2007); Phys. Lett. B **651**, 119 (2007).
[27] M. Mishra and C. P. Singh, Phys. Rev. C **78**, 024910 (2008).
[28] M. Cheng *et al.*, Phys. Rev. D **81**, 054504 (2010); M. Cheng *et al.*, Phys. Rev. D **77**, 014511 (2008).
[29] C. Schmidt, Nucl. Phys. A **A820** 41c (2009).
[30] Z. Fodor and S. D. Katz, J. High Energy Phys. 04 (2004) 050.
[31] S. Ejiri, C. R. Alton, S. J. Hands, O. Kaczmarek, F. Karsch, E. Laermann, and C. Schmidt, Prog. Theor. Phys. Suppl. **153**, 118 (2004).
[32] N. G. Antoniou and A. S. Kapoyannis, Phys. Lett. B **563**, 165 (2003).
[33] N. G. Antoniou, F. K. Diakonos, and A. S. Kapoyannis, Nucl. Phys. **A759**, 417 (2005).
[34] A. Barducci, R. Casalbuoni, G. Pettini, and R. Gatto, Phys. Rev. D **49**, 426 (1994).
[35] A. Barducci, G. Pettini, L. Ravagli, and R. Casalbuoni, Phys. Lett. B **564**, 217 (2003).
[36] D. Zschiesche *et al.*, J. Phys. G **31**, 935 (2005).
[37] P. Costa, M. C. Ruivo, and C. A. deSousa, Phys. Rev. D **77**, 096001 (2008).
[38] M. Ciminale, R. Gatto, N. D. Ippolito, G. Nardulli, and M. Ruggieri, Phys. Rev. D **77**, 054023 (2008).
[39] P. Costa, C. A. deSousa, M. C. Ruivo, and H. Hansen, Europhys. Lett. **86**, 31001 (2009).
[40] M. Asakawa and K. Yazaki, Nucl. Phys. **A504**, 668 (1989).
[41] J. Berges and K. Rajagopal, Nucl. Phys. **B538**, 215 (1999).
[42] O. Scavenius, A. Mocsy, I. N. Mishustin, and D. H. Rischke, Phys. Rev. C **64**, 045202 (2001).
[43] K. Kashiwa, H. Kouno, M. Matsuzaki, and M. Yahiro, Phys. Lett. B **662**, 26 (2008).
[44] S. Rößner, C. Ratti, and W. Weise, Phys. Rev. D **75**, 034007 (2007).
[45] M. A. Halasz, A. D. Jackson, R. E. Shrock, M. A. Stephanov, and J. J. M. Verbaarschot, Phys. Rev. D **58**, 096007 (1998).
[46] Y. Hatta and T. Ikeda, Phys. Rev. D **67**, 014028 (2003).
[47] R. A. Lacey *et al.*, Phys. Rev. Lett. **98**, 092301 (2007).
[48] J. W. Chen, K. Fukushima, H. Kohiyama, K. Ohnishi, and U. Raha, Phys. Rev. D **80**, 054012 (2009).
[49] P. Castorina, R. Redlich, and H. Satz, Eur. Phys. J. C **59**, 67 (2009).